Formation of localized structures in the Peyrard–Bishop–Dauxois model

2008 J. Phys.: Condens. Matter 20 415104

(http://iopscience.iop.org/0953-8984/20/41/415104)

IOP Publishing Journal of Physics: Condensed Matter

J. Phys.: Condens. Matter **20** (2008) 415104 (9pp) doi:10.1088/0953-8984/20/41/415104

Formation of localized structures in the Peyrard–Bishop–Dauxois model

Conrad B Tabi[1], Alidou Mohamadou[1,2,3] and Timoléon C Kofané[1,3]

[1] Laboratory of Mechanics, Department of Physics, Faculty of Science, University of Yaounde I, PO Box 812, Yaounde, Cameroon
[2] Condensed Matter Laboratory, Department of Physics, Faculty of Science, University of Douala, PO Box 24157, Douala, Cameroon
[3] The Abdus Salam International Center for Theoretical Physics, PO Box 586, Strada Costiera 11, I-34014 Trieste, Italy

E-mail: contab408@yahoo.com, mohdoufr@yahoo.fr and tckofane@yahoo.com

Received 6 February 2008, in final form 13 August 2008
Published 5 September 2008
Online at stacks.iop.org/JPhysCM/20/415104

Abstract

We explore in detail the properties of modulational instability (MI) and the generation of soliton-like excitations in DNA nucleotides. Based on the Peyrard–Bishop–Dauxois (PBD) model of DNA dynamics, which takes into account the interaction with neighbors in the structure, we derive through the semidiscrete approximation a modified discrete nonlinear Schrödinger (MDNLS) equation. From this equation, we predict the condition for the propagation of modulated waves through the system. To verify the validity of these results we have carried out numerical simulations of the PBD model and the initial conditions in the form of planar waves whose modulated amplitudes are given by the examples studied in the MDNLS equation. In the simulations we have found that a train of pulses are generated when the lattice is subjected to MI, in agreement with the analytical results obtained in an MDNLS equation. Also, the effects of the harmonic longitudinal and helicoidal constants on the dynamics of the system are notably pointed out. The process of energy localization from a nonsoliton initial condition is also explored.

(Some figures in this article are in colour only in the electronic version)

1. Introduction

Nonlinear excitations (solitons, discrete breathers, intrinsic localized modes, etc) have been drawing increasing attention over recent years and are widely believed to be responsible for several effects in molecular chains, such as charge and thermal conductivity, energy transfer and localization, etc [1]. A particular interesting discrete system that support solitons and localized modes is deoxyribonucleic acid, or DNA. In this system, localization of energy has been suggested as a precursor of the transcription bubble [2, 3], and moving localized oscillations as a method of transport of information along the double strand [4].

The idea that nonlinear excitations could play a role in the dynamics of DNA has become increasingly popular. Englander *et al* [5] first suggested a theory of soliton excitations as an explanation of the open states of DNA. Later Yamosa [6] proposed another soliton theory using a planar base-rotator model that was further refined by Takeno and Homma [7], who introduced a model allowing some discreteness effects to be taken into account, and by Zhang [8], who improved the model for base coupling. Among the processes that have been described using bubbles and solitary waves one can find the following: the binding of specific enzymes to DNA (e.g. DNA polymerases, recombinases, helicases or RNA polymerases) and the thermal evolution of enzyme-created bubbles [9], the displacement of a bubble from the promoter to the coding regions [4, 10, 11], the process of energy collection in the active regions under enzyme action [12, 13] and the opening of bubbles at the start sites of transcription [14, 15]. The use of localized structure bubble-like structures in explaining these phenomena sets the problem of their creation and stability.

In order to explain some aspects of DNA dynamics, a great number of mathematical models have been proposed [10, 16].

Yakushevich has proposed a model [10, 16] to describe the DNA dynamics. This model was further improved by Gaeta [17]. The Yakushevich model takes into account only the unzipping of the helical structure. Another interesting approach has been followed by Peyrard and Bishop (PB model) [2], who proposed a model in order to study the dynamics and thermodynamics of base pair opening in DNA denaturation and transcription. In this model, the double strand is equivalent to the Klein–Gordon chain, the variables are the distances between nucleotides within each base pair, and only short-range interactions due to the stacking coupling are considered. Other DNA models ignore these kinds of interactions and only consider long-range interactions, whose origin lies in the dipole moments that characterize the hydrogen bonds between the nucleotides [18]. The PB model was later improved by Dauxois, Peyrard and Bishop [19–21]. Many authors have shown that the most standard mechanism through which bright solitons or solitary wave structures appear is through the activation of modulational instability (MI) of plane waves [22]. For this instability, a specific range of wavenumbers of plane-wave profiles becomes unstable to modulations, leading to an exponential growth of the unstable modes and eventually to delocalization (upon excitation of such wavenumbers) in momentum space. That is equivalent to delocalization in position space, and hence the formation of localized, coherent solitary wave structures [23]. In the above-mentioned contexts, MI has been suggested to be responsible for energy-localization mechanisms leading to the formation of large-amplitude nonlinear excitations in hydrogen-bonded crystals or DNA molecules [2, 24]. So, it is important and worthwhile to study the properties of the MI in a nonlinear medium, especially in DNA.

In what follows, we will focus on the effects of the harmonic constants of the longitudinal and the helicoidal springs on the PBD model. Particular attention will be paid to the competition of these two parameters in the generation of the solitonic structures through MI. Also, the energy of localization will be studied. Indeed, in the context of the 'traditional' NLS equation, perhaps the most standard mechanism through which bright solitons and solitary wave structures appear is through the activation of the MI of plane waves. The MI is a general feature of continuum as well of discrete nonlinear wave equations and its demonstration spans a diverse set of disciplines, ranging from plasma physics [25], electrical transmission lines [26], nonlinear optics [27] and DNA molecule [22, 24], to cite just a few.

The rest of the paper is outlined as follows. After briefly reviewing (in section 2) the PBD model, we will derive the equation describing the propagation of modulated waves in the molecule (the MDNLS equation), then through the standard linear stability analysis, the MI criterion will be presented as well as the threshold amplitude. In section 3, we perform numerical experiments in order to confirm analytical predictions and excellent agreement is obtained. Section 4 is devoted to some concluding remarks.

2. The discrete nonlinear equation for the dynamics and stability analysis

2.1. The discrete nonlinear equation for the dynamics of the PBD model

The PB model has been used to study the processes of transcription and replication as well as to describe thermal denaturation of DNA molecule. The first model, elaborated in 1989 [2], only considers short-range interactions due to the stacking of adjacent base pairs. According to the PBD model [2, 19–21], the DNA chain is treated as a perfectly periodic structure with lattice period l. This means that the masses of all the nucleotides and the corresponding interaction parameters are assumed to be equal [6, 14]. This was extensively elaborated in [21]. The PBD model takes only transversal motions into consideration as well as the nearest-neighbor harmonic interaction along the DNA chain. Since the bases are connected one to another through hydrogen bonds, the Morse potential is chosen because of its shape. Let y_n and z_n be the transversal displacements of the nucleotides of different strands at site n from their equilibrium positions. Basically important helicoidal structure is taken into account through the harmonic interaction of the nucleotides having the coordinates y_n and $z_{n\pm h}$ [28]. Inasmuch as the helix has a corresponding pitch of about 10 base pairs per turn, we assume $h = 4$ [28, 29]. The Hamiltonian of the system is written as follows [2, 21, 28]:

$$H = \sum_{n=1}^{N}\Bigg[\frac{m}{2}(\dot{y}_n^2 + \dot{z}_n^2) + \frac{S_1}{2}[(y_n - y_{n-1})^2 + (z_n - z_{n-1})^2] + \frac{S_2}{2}[(y_n - z_{n+h})^2 + (y_n - z_{n-h})^2] + V(y_n - z_n)\Bigg]. \quad (1)$$

Here S_1 and S_2 are the harmonic constants of the longitudinal and helicoidal springs, respectively. The on-site potential, announced to be the Morse one, takes the form $V(y_n - z_n) = D[\mathrm{e}^{-a(y_n - z_n)} - 1]^2$, where D is the dissociation energy and a is a parameter homogeneous to the inverse of a length, which sets the spatial scale of the potential. It is convenient to use the coordinates r_n and u_n for in-phase and out-of-phase motions, defined as

$$r_n = (y_n + z_n)/\sqrt{2}, \qquad u_n = (y_n - z_n)/\sqrt{2}. \quad (2)$$

Obviously, r_n describes the movement of the center of mass of the nucleotide pair at site n, while u_n represents the stretching of the pair. According to equations (1) and (2), we can straightforwardly obtain two perfectly decoupled equations of motion, linear for r_n and nonlinear for u_n:

$$m\ddot{r}_n = S_1(r_{n+1} + r_{n-1} - 2r_n) + S_2(r_{n+h} + r_{n-h} - 2r_n) \quad (3)$$

$$m\ddot{u}_n = S_1(u_{n+1} + u_{n-1} - 2u_n) - S_2(u_{n+h} + u_{n-h} + 2u_n) + 2\sqrt{2}aD\,\mathrm{e}^{-a\sqrt{2}u_n}(\mathrm{e}^{-a\sqrt{2}u_n} - 1). \quad (4)$$

In this work, we are interested in the out-of-phase equation, because it describes nonlinear waves, whereas the in-phase equation describes linear waves (phonons). Expanding the terms in the exponential, we get

$$\ddot{u}_n = K_1(u_{n+1} + u_{n-1} - 2u_n) - K_2(u_{n+h} + u_{n-h} + 2u_n) - \omega_{\mathrm{g}}^2(u_n + \alpha u_n^2 + \beta u_n^3) \quad (5)$$

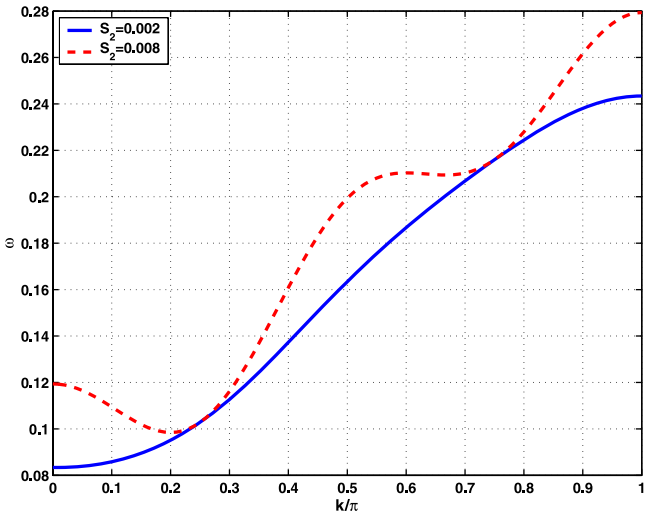

Figure 1. The linear dispersion relation $\omega = \omega(k)$. $S_1 = 0.04$ eV Å^{-2}, $D = 0.15$ eV, and $a = 6.3$ Å^{-1}. The solid curve is plotted for $S_2 = 0.0025$ eV Å^{-2} and the dashed one for $S_2 = 0.01$ eV Å^{-2}.

where $K_1 = \frac{S_1}{m}$, $K_2 = \frac{S_2}{m}$, $\omega_g^2 = \frac{4a^2D}{m}$, $\alpha = -\frac{3a}{\sqrt{2}}$ and $\beta = \frac{7a^2}{3}$. The geometrical parameters of the model can be straightforwardly fixed according to the available structural data [30]. We selected values similar to those previously considered for the fixed planes case, which have been discussed elsewhere: the choice of the S_1 parameter can be independently derived [31] from the twist persistence length [32], while the choice of the other two parameters was based [31] on a comparison with mechanical denaturation experiments [32]. In particular, the important parameter D, which sets the main energy scale, has been tuned to reproduce as closely as possible the experimental value of the denaturation temperature $T_D = 350$ K. The values of the parameters are $m = 300$ amu, $S_1 = 0.04$ eV Å^{-2}, $D = 0.15$ eV and $a = 6.3$ Å^{-1} [31, 33].

The appropriate linear dispersion relation, which is optical in the present case, is described by the following relation:

$$\omega^2 = \omega_g^2 + 4K_1 \sin^2\left(\frac{k}{2}\right) + 4K_2 \cos^2\left(\frac{kh}{2}\right). \qquad (6)$$

Figure 1 plots the above dispersion relation versus the wavenumber k and we note different behaviors in the dynamics of the base pairs with respect to the parameter S_2. In figure 1, the linear spectrum has a gap $\omega_{01} = (\omega_g^2 + 4K_2)^{1/2}$ and an upper cutoff frequency $\omega_{max} = (\omega_g^2 + 4K_1 + 4K_2)^{1/2}$. As one increases the parameters S_2, the dispersion curve oscillates (dashed curve). This behavior is probably induced by the competition between the longitudinal and helicoidal spring constants (which becomes more important in this case). In the rest of this paper, we assume that the gap angular frequency ω_g is larger than other frequencies present in the system, that is $\omega_g^2 \gg 4(K_1 + K_2)$, so that any frequency mixing should be avoided.

Several approaches are used nowadays to derive a DNLS equation in nonlinear physical systems. The one used by Kivshar and Peyrard [34] can be extended here but, since the Morse potential is nonsymmetric, the method used by Daumont *et al* [35] is more appropriate. In fact, it takes into consideration the first harmonics and introduces a few functions $F_{j,n}$, which bring out the importance of nonlinear parameters. We then substitute into equation (5) the trial solution

$$u_n(t) = F_{1,n}(t)\, e^{-i\omega_g t} + F_{0,n}(t) + F_{2,n}(t)\, e^{-2i\omega_g t} + \text{c.c.} \quad (7)$$

The coefficients of $e^{-i\omega_g t}$ lead to the following one-dimensional MDNLS equation:

$$i\frac{dF_{1,n}}{dt} + P(F_{1,n+1} + F_{1,n-1} - 2F_{1,n}) + R(F_{1,n+h} + F_{1,n-h} + 2F_{1,n}) + Q|F_{1,n}|^2 F_{1,n} = 0 \qquad (8)$$

where P, R and Q are given by

$$P = \frac{K_1}{2\omega_g} \qquad R = -\frac{K_2}{2\omega_g} \qquad Q = \frac{\omega_g}{2}\left(\frac{10\alpha^2}{3} - 3\beta\right). \qquad (9)$$

The NLS equation is among the most important physical models in the field of nonlinear waves. Besides its fundamental value as a first-order nonlinear wave equation, it is a nonintegrable model in the one-dimensional case [36] and represents many different physical systems: from laser wavepackets propagating in nonlinear material to matter waves in Bose–Einstein condensates, gravitational models for quantum mechanics, plasma physics or wave propagation in geological systems, among others [37–39]. Here, one sees that equation (8) is a general physical model which may have applications to DNA. From equation (8), when $S_2 = 0$, one obtains the well known DNLS equation.

2.2. Linear stability analysis

We begin our analysis by considering the linear dispersion properties of an MDNLS equation. To do so, we write $F_{1,n}(t) = \phi_0\, e^{i(kn-\omega_0 t)}$, where the wavenumber k, the angular frequency ω_0 and the amplitude ϕ_0 satisfy the dispersion relation:

$$\omega_0 = 4P \sin^2\left(\frac{k}{2}\right) + 4R \cos^2\left(\frac{kh}{2}\right) - Q|\phi_0|^2. \qquad (10)$$

To examine the linear stability of the initial plane waves, we look for a solution of the form

$$F_{1,n}(t) = \phi_0[1 + B_n(t)]\, e^{i(kn-\omega_0 t)} \qquad (11)$$

where the perturbation amplitude $B_n(t)$ is assumed to be small in comparison with the carrier wave amplitude ϕ_0. The perturbation $B_n(t)$ verifies the following relation:

$$i\dot{B}_n + P[(B_{n+1} + B_{n-1} - 2B_n)\cos(k) + i(B_{n+1} - B_{n-1})\sin(k)] + R[(B_{n+h} + B_{n-h} - 2B_n)\cos(kh) + i(B_{n+h} - B_{n-h})\sin(kh)] + Q|\phi_0|^2(B_n + B_n^*) = 0. \qquad (12)$$

Furthermore, assuming a general solution of the above-mentioned system of the form

$$B_n(t) = B_1\, e^{i(Kn-\Omega t)} + B_2^* e^{-i(Kn-\Omega^* t)} \qquad (13)$$

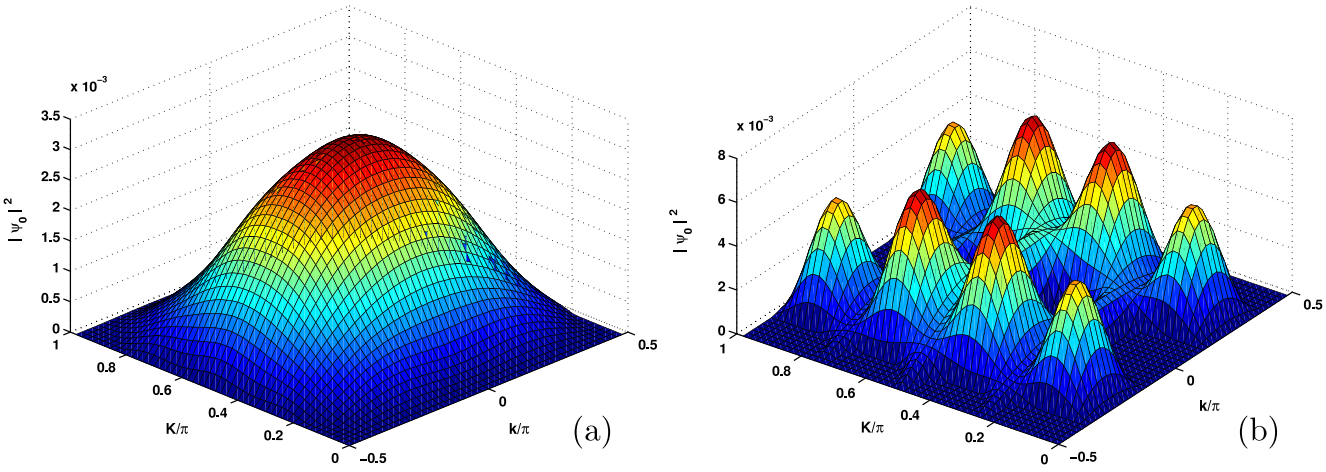

Figure 2. The threshold amplitude: (a) $S_2 \leqslant S_{2,\mathrm{cr}}$ and (b) $S_2 > S_{2,\mathrm{cr}}$.

where the asterisk denotes complex conjugation, K and Ω represent, respectively, the wavenumber and the angular frequency of the perturbation amplitude, and B_1 and B_2 are complex constant amplitudes. Inserting equation (13) into equation (12) and after linearization around the unperturbed plane wave, we obtain the linear homogeneous system for B_1 and B_2:

$$\begin{pmatrix} a_{11}+\Omega & a_{12} \\ a_{21} & a_{22}-\Omega \end{pmatrix} \begin{pmatrix} B_1 \\ B_2 \end{pmatrix} = \begin{pmatrix} 0 \\ 0 \end{pmatrix}. \tag{14}$$

The condition for the existence of nontrivial solutions of this linear homogeneous system is given by a second-order equation for the frequency Ω, that is

$$\Omega^2 + (a_{11}-a_{22})\,\Omega + a_{12}a_{21} - a_{11}a_{22} = 0 \tag{15}$$

with

$$\begin{aligned} a_{11} &= -2P[\sin(K)\sin(k) - (\cos(K)-1)\cos(k)] \\ &\quad - 2R[\sin(Kh)\sin(kh) - (\cos(Kh)-1)\cos(kh)] \\ &\quad + Q|\phi_0|^2 \\ a_{12} &= a_{21} = Q|\phi_0|^2 \\ a_{22} &= 2P[\sin(K)\sin(k) + (\cos(K)-1)\cos(k)] \\ &\quad + 2R[\sin(Kh)\sin(kh) + (\cos(Kh)-1)\cos(kh)] \\ &\quad + Q|\phi_0|^2. \end{aligned}$$

Equation (15) can be rewritten as

$$\begin{aligned} (\Omega_1)^2 &= (\Omega - 2P\sin(K)\sin(k) - 2R\sin(Kh)\sin(kh))^2 \\ &= 8\left[P\sin^2\left(\frac{K}{2}\right)\cos(k) + R\sin^2\left(\frac{Kh}{2}\right)\cos(kh)\right] \\ &\quad \times\left[2P\sin^2\left(\frac{K}{2}\right)\cos(k) + 2R\sin^2\left(\frac{Kh}{2}\right)\cos(kh)\right. \\ &\quad \left. - Q|\phi_0|^2\right]. \end{aligned} \tag{16}$$

An instability will be developed in the molecule if the right-hand side of this equation becomes negative, i.e. the perturbed wave is unstable only if

$$\begin{aligned} &\left[P\sin^2\left(\frac{K}{2}\right)\cos(k) + R\sin^2\left(\frac{Kh}{2}\right)\cos(kh)\right] \\ &\quad \times\left[2P\sin^2\left(\frac{K}{2}\right)\cos(k) + 2R\sin^2\left(\frac{Kh}{2}\right)\cos(kh)\right. \\ &\quad \left. - Q|\phi_0|^2\right] < 0. \end{aligned} \tag{17}$$

Equation (17) is the MI criterion of our system. The above MI criterion gives us the possibility to express the initial amplitude $|\phi_0|$ as a function of the threshold amplitude $|\phi_{0,\mathrm{cr}}|$. Therefore, a plane wave introduced in the system becomes unstable if the initial amplitude $|\phi_0|$ exceeds the threshold amplitude $|\phi_{0,\mathrm{cr}}|$ defined as follows:

$$\begin{aligned} |\phi_0|^2 \geqslant |\phi_{0,\mathrm{cr}}|^2 &= \frac{2}{Q}\left[P\sin^2\left(\frac{K}{2}\right)\cos(k)\right. \\ &\quad \left. + R\sin^2\left(\frac{Kh}{2}\right)\cos(kh)\right]. \end{aligned} \tag{18}$$

In the long-wavelength limit, when $k \ll 1$ and $K \ll 1$, we deduce from the above threshold amplitude that

$$\frac{PK^2 + RK^2h^2}{4} \geqslant 0 \Longrightarrow S_2 \leqslant S_{2,\mathrm{cr}} = \frac{S_1}{h^2}. \tag{19}$$

Figure 2 shows how the value of the threshold amplitude $|\psi_0|$ depends on the helicoidal spring constant S_2. In fact, when the helicoidal spring constant S_2 is lower than $S_{2,\mathrm{cr}}$ we have only one satellite side band (see figure 2(a)). But, when $S_2 > S_{2,\mathrm{cr}}$, we observe an explosion of the threshold amplitude into satellite side bands (see figure 2(b)). One can say that, as the coefficient of the helicoidal coupling becomes important, there is an explosion of the instability domain. We also note that the magnitude of the threshold amplitude has increased in this case, predicting, indubitably, an increase of the amplitude under modulation, which causes large oscillations of the cells.

Let us remark that, when we set $k = 0$, there are two cases.

- For $|\psi_0|^2 < |\psi_{0,\mathrm{cr}}|^2$ and $S_2 \leqslant S_{2,\mathrm{cr}}$, the waves are unstable with respect to any modulation as shown in figure 3(a) (solid line) in the interval $K \in [0, \pi/2]$

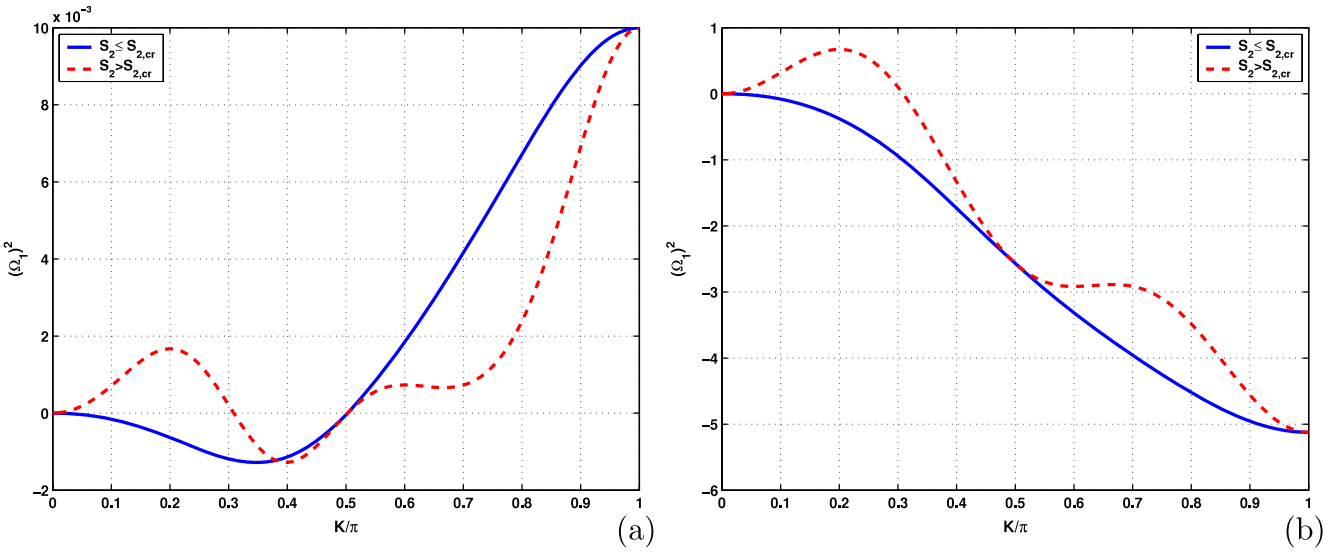

Figure 3. Variation versus K of $(\Omega_1)^2 = (\Omega - 2P\sin(K)\sin(k) - 2R\sin(Kh)\sin(kh))^2$ for the modulation waves ($k = 0$) as the wave crosses the critical value $|\psi_{0,\mathrm{cr}}|$: (a) $|\psi_0|^2 < |\psi_{0,\mathrm{cr}}|^2$ and (b) $|\psi_0|^2 > |\psi_{0,\mathrm{cr}}|^2$.

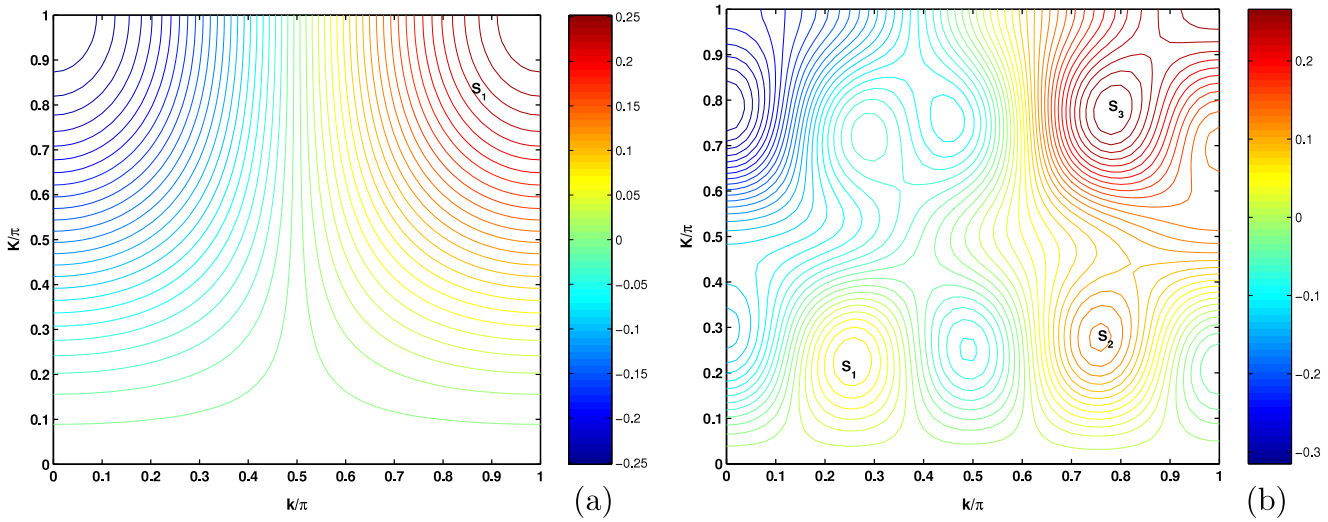

Figure 4. Regions of modulational instability/stability $(\Omega_1)^2 = (\Omega - 2P\sin(K)\sin(k) - 2R\sin(Kh)\sin(kh))^2$ for $|\psi_0|^2 < |\psi_{0,\mathrm{cr}}|^2$: (a) $S_2 \leqslant S_{2,\mathrm{cr}}$, (b) $S_2 > S_{2,\mathrm{cr}}$.

and, for $S_2 > S_{2,\mathrm{cr}}$, the system may be in the interval $[3\pi/10, \pi/2]$. For the same case, wave instability is predicted in $[3\pi/10, \pi/2]$ as shown in figure 3(a) (dashed line).

- For $|\psi_0|^2 > |\psi_{0,\mathrm{cr}}|^2$, there is a marginal instability as depicted in figure 3(b) (solid curve), as $S_2 \leqslant S_{2,\mathrm{cr}}$, but, for $S_2 > S_{2,\mathrm{cr}}$, the stability region depicted in the case $|\psi_0|^2 < |\psi_{0,\mathrm{cr}}|^2$ is still present (dashed curve). Figure 4 presents the diagram of instability/stability in the (k, K) plane. Figure 4(a) shows for the case $S_2 \leqslant S_{2,\mathrm{cr}}$ that the molecule is stable in the region ($k \in [0.6\pi, \pi]$, $K \in [0.4\pi, \pi]$) labeled around the point S_1. Next, for $S_2 > S_{2,\mathrm{cr}}$ the molecule presents three points (S_1, S_2, S_3) around which the system is stable as viewed in figure 4(b).

3. Numerical investigations

According to the analytical results discussed in section 2, the stability of a plane wave with wavenumber k modulated by a small-amplitude wave of wavenumber K is determined by the instability criterion (17). When this relation is fulfilled, we expect that the system exhibits an instability as predicted analytically, which leads to the self-induced modulation of an input plane wave with the subsequent generation of localized pulses [22–27, 34, 35]. Thus, it becomes of interest to investigate the nature of formation of different wave patterns that may arise by the MI process in the PBD model of a DNA molecule during the evolution of the initial waves through the system. However, the linear stability analysis has been obtained through an MDNLS equation, which is only

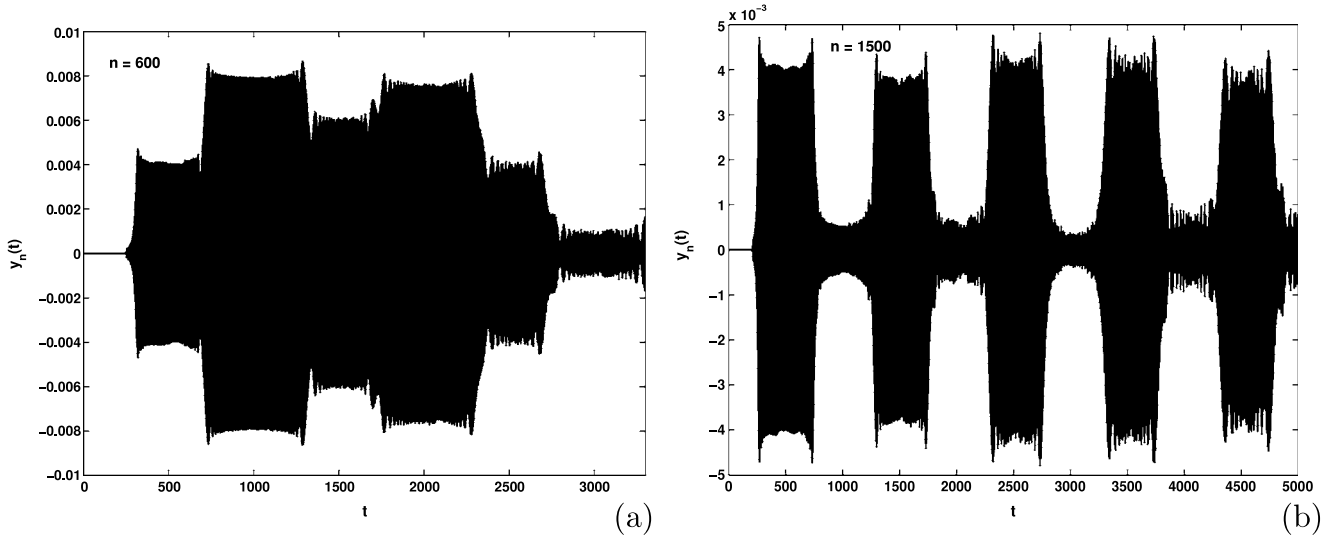

Figure 5. Dynamics of modulated waves as a function of time (t.u.) showing the MI of slowly modulated plane waves for $S_2 \leqslant S_{2,\mathrm{cr}}$. (a) Soliton-like objects in the molecule at base pair 600; (b) soliton-like objects in the molecule at base pair 1500.

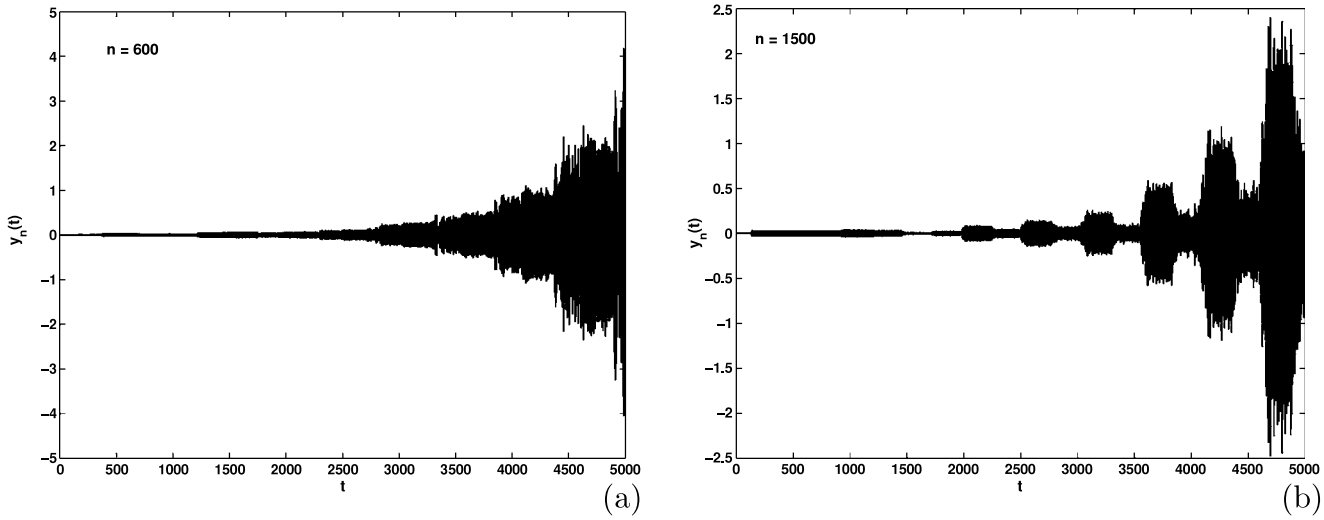

Figure 6. Dynamics of modulated waves as a function of time (t.u.) showing the MI of slowly modulated plane waves for $S_2 > S_{2,\mathrm{cr}}$; (a) soliton-like objects in the molecule at base pair 600; (b) soliton-like objects in the molecule at base pair 1500.

an approximate description of the equation of motion (4). Consequently, the linear stability analysis can only detect the onset of instability. In order to check the validity of our analytical approach and to determine the evolution of the system beyond the instability point, we have performed numerical simulations of the equation of motion (4) with a given initial condition. The system has been integrated with a fourth-order Runge–Kutta scheme with a timestep chosen to conserve the energy to an accuracy better than 0.005. The number of base pairs is chosen in order to avoid wave reflection at the end of the molecule. We chose as an initial condition a linear wave with a slightly modulated amplitude:

$$u_n(t=0) = \phi_0[1 + 0.01\cos(Kn)]\cos(kn). \qquad (20)$$

We have chosen $\phi_0 = 0.5$, $k = 0.2\pi$ and $K = 0.4\pi$. When the effects of the first neighbors are more important in the system $S_2 \leqslant S_{2,\mathrm{cr}}$, according to figure 4(a) the corresponding point labeled by ($k = 0.2\pi, K = 0.4\pi$) lies in the instability zone. Therefore, we expect the modulated wave to be unstable. The time evolution of the initial wave launched through the system can be viewed in figure 5 for the base pairs 600 and 1500, respectively. As predicted by the analytical results the initial wave is disintegrated into a train of pulses. Figure 5(a) presents the propagation of the wave at base pair 600. At this base pair, one sees that the initial wavepacket disintegrates progressively as time increases. Further, at base pair 1500 we obtain the same phenomena. But here, the wavepacket disintegrates with an uniform amplitude and wavelength. When the effects of neighbors become more important in the system ($S_2 > S_{2,\mathrm{cr}}$), one obtains the results depicted in figure 6 at the same base pair. From figure 4(b), we see that the corresponding point ($k = 0.2\pi, K = 0.4\pi$)

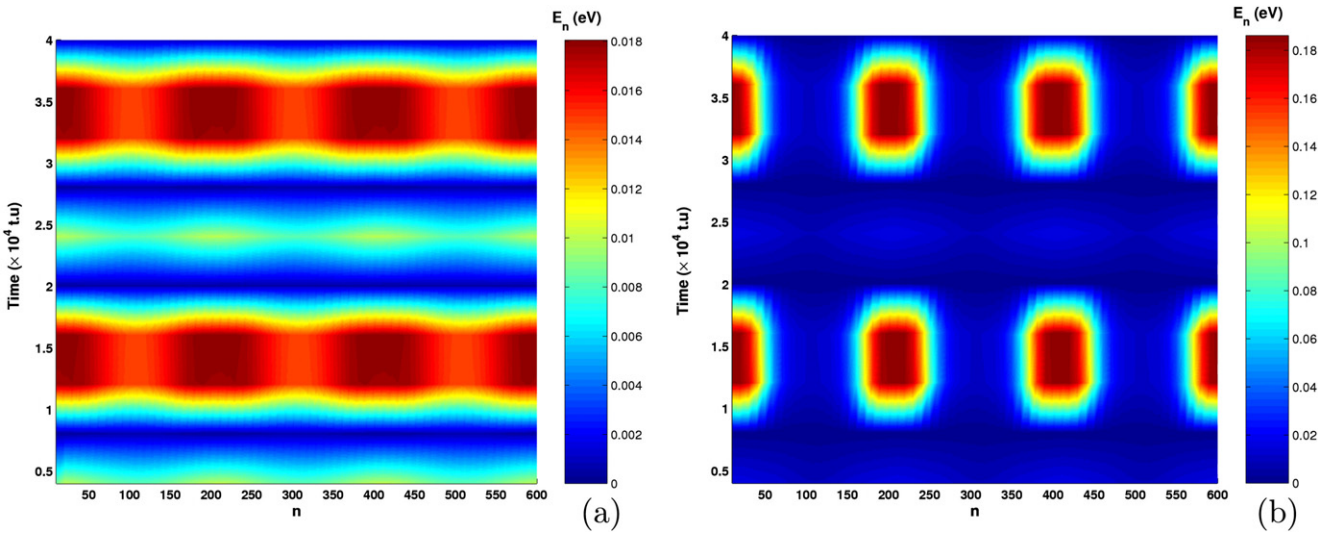

Figure 7. Energy localization (a) $S_2 \leqslant S_{2,\mathrm{cr}}$; (b) $S_2 > S_{2,\mathrm{cr}}$.

is also located in the instability zone. One sees that the initial wave predicted to be unstable against the modulation break up into a pulse train. But the amplitude of waves increases as the time increases. We just see that, when the MI conditions are fulfilled, due to the balance between nonlinearity and dispersion, the initial wave breaks into pulse trains. The solitonic excitation of the pulse train has envelope functions with a familiar shape of the theory of soliton-like objects. Each element of the train has the shape of a soliton-like object. But, in contrast to solitons, they emerge as a solution of a time-dependent classical equation of motion. It was suggested a long time ago that solitons could be used to carry data at a very high rate, because of their ability to overcome the dispersion limitation through a balance between the self-phase modulation and dispersion effects [40]. In fact, soliton pulses are known to have many other desirable properties, such as their robustness against small changes in the pulse shape or amplitude around the exact soliton profile leading to treat such changes only as small perturbations on soliton propagation. The existence of discrete breathers in the PB model of DNA has been suggested by Dauxois [28, 29]. Afterward, numerical simulations performed by Dauxois [29, 33] suggested that localized oscillations can be precursors of bubbles that appear in the thermal denaturation of DNA.

To study the localization of energy in the PBD model, we would look for a solution for which at least a part of the initial energy is stored in permanent localized structures. Indeed, when the MI conditions are fulfilled in a system, one can obtain a localized concentration of energy. In this sense, Daumont [35] and coworkers [41] have shown that the discreteness of the system causes the instability of the extended solutions. They tend to self-modulate evolving to localized soliton-like modes that interact nonelastically and grow the largest ones at the expense of the smallest [42]. It gives a possible path to the collecting of energy. Thermal fluctuations, which exist in the molecule due to the physiological temperature, are shown to be a pathway to energy localization and formation of localized structures [41, 43]. We have studied the energy of localization through the density of energy given by

$$E_n = \tfrac{1}{2}m\dot{u}_n^2 + \tfrac{1}{2}S_1[(u_n - u_{n-1})^2 + (u_{n+1} - u_n)^2] + \tfrac{1}{2}S_2[(u_n + u_{n-h})^2 + (u_{n+h} + u_n)^2] + D(\mathrm{e}^{-a\sqrt{2}u_n} - 1)^2. \quad (21)$$

With the conditions of figure 5 ($S_2 < S_{2,\mathrm{cr}}$, $k = 0.2\pi$, $K = 0.4\pi$), we know that the system is modulationally unstable and we have obtained the formation of localized structures in the molecule. Given a nonsoliton initial condition (20), the system can group some of the energy in soliton-like structures (see figure 6) while the rest of the energy is spread in the form of radiation, as shown in figure 7(a). Then, after a transient time, we will again have a robust localization of energy in the system. In this case, the energy is located along all the base pairs and for some specific time. But, for ($S_2 > S_{2,\mathrm{cr}}$, $k = 0.2\pi$, $K = 0.4\pi$) which is the case of figure 6, one can see from figure 7(b) that the energy is effectively localized in some particular sites of the molecule. We also remark that this localization of energy has happened with a certain spatiotemporal recurrence. From figures 5, 6 and 7 one can really say that the present process of localization of energy is linked to the MI process.

4. Conclusion

In the framework of the PBD model of a DNA molecule, we have shown, using the so-called semidiscrete approximation, that an MDNLS equation is a general physical model which may have application to DNA dynamics. Through the linear stability analysis, we have predicted the existence of soliton-like structures in the DNA molecule. We have obtained that, for $S_2 < S_{2,\mathrm{cr}}$, one retrieves the results obtained by Kivshar and Peyrard [34] for a standard DNLS equation (see figure 3). The most interesting feature comes from the case $S_2 > S_{2,\mathrm{cr}}$, where both the amplitude and regions of MI change considerably (figures 2(b), 3 and 4(b)). There is an explosion of side

bands when the helicoidal spring constant is greater than the longitudinal one.

Numerical experiments have been carried out in order to confirm the analytical predictions. It has been observed that, in the case where $S_2 \leqslant S_{2,\mathrm{cr}}$, there is an MI since the initial modulated plane wave breaks into a train of pulses and soliton-like objects. Their amplitude, in comparison to the frustrated case ($S_2 > S_{2,\mathrm{cr}}$), is small. This can be analyzed as the action of the waves flowing in the molecule and which plays an important role in the conformational concerns taking place in the B-DNA molecule. On the other hand, the increase in the amplitude of the wave trains due to frustration mainly describes the action of RNA polymerase which breaks progressively the hydrogen bonds for the messenger RNA to come and copy the genetic code. We believe that the existence and formation of solitons in the DNA molecule could be a proper candidate to explain how data are exchanged during basic biological phenomena such as transcription and replication. As is well known, for the hydrogen bond to be broken, there should be a concentration of the enzyme and of the energy brought through the hydrolysis of ATP. This explains the form of figure 6, which at the beginning of the wave propagation is thin and has their amplitudes increased. More precisely, this is the interaction between DNA and RNA polymerase when DNA opens locally. In need of clarity, the energy density has been represented and, as a first remark, the quantity of energy involved is, in the unfrustrated case, low compared to the energy involved in the frustrated case. There is also effective energy localization in the second case, so as to indicate the importance of frustration in the local opening of DNA strands. This has been pointed out by Kapri *et al* [44] who studied the force-induced first-order transition in the DNA lattice model. According to those authors, fluctuating force unzips DNA by a gradual increase of bubble size. This is only possible if the various energy releasers concentrate on specific sites without fluctuating back and forth with, as a result, unzipping and then breaking the strong hydrogen bonds. In our opinion, there is more to explore in the B-DNA model in the way one could carry out the influence of resonance mode on energy and information transfer in DNA. There would be a great deal of interest in looking at the two-component case, since in real DNA, the two strands are different but complementary.

Acknowledgments

AM and TCK acknowledge the invitation of the Condensed Matter and Statistical Physics Section (CMSPS), of the Abdus Salam International Center for Theoretical Physics (ICTP), during which this work was finalized.

References

[1] Reiss C 1994 *Nonlinear Excitations in Biomolecules* ed M Peyrard (Les Ulis: Springer)
[2] Peyrard M and Bishop A R 1989 *Phys. Rev. Lett.* **62** 2755
Goldar A, Thonson H and Seddon J M 2008 *J. Phys.: Condens. Matter* **20** 035102
[3] Dauxois T, Peyrard M and Willis C R 1992 *Physica* D **57** 267
[4] Salerno M and Kivshar Y S 1994 *Phys. Lett.* A **193** 263
[5] Englander S W, Kallenbach N R, Heeger A J, Krumhasnl J A and Kitwin S 1980 *Proc. Natl Acad. Sci. USA* **777** 7222
[6] Yomosa S 1983 *Phys. Rev.* A **27** 2120
Yomosa S 1984 *Phys. Rev.* **30** 474
[7] Takeno S and Homma S 1987 *Prog. Theor. Phys.* **77** 548
[8] Chun-Ting Z 1987 *Phys. Rev.* A **35** 886
[9] Henning D, Archilla J R F and Romero J M 2005 *J. R. Soc. Interface* **2** 89
[10] Campa A 2001 *Phys. Rev.* E **63** 021901
Yakushevich L V 2004 *Nonlinear Physics of DNA* 2nd edn (Chichester: Wiley)
[11] Cuenda S, Sanchez A and Quintero N R 2006 *Physica* D **223** 214
Lennholm E and Hornquist M 2003 *Physica* D **177** 233
[12] Julian J-L Ting and Peyrard M 1996 *Phys. Rev.* E **53** 1011
Forinash K, Peyrard M and Malomed B A 1994 *Phys. Rev.* E **49** 3400
[13] Cuevas J, Palmero F, Archilla J R and Romero J 2002 *J. Phys. A: Math. Gen.* **35** 10519
Dauxois T, Peyrard M and Willis C R 1992 *Phys. Rev.* E **48** 4768
[14] Kalosakas G, Rasmussen O, Bishop A R, Cnoi C H and Usheva A 2004 *Europhys. Lett.* **68** 127
Ares S and Kalasakas G 2007 *Nano Lett.* **7** 307
[15] Rapti Z, Smerzi A, Rasmussen O, Bishop A R, Cnoi C H and Usheva A 2006 *Phys. Rev.* E **73** 051902
[16] Yakushevich L V 1989 *Phys. Lett.* A **136** 413
Yakushevich L V, Savin A V and Manevitch L I 2002 *Phys. Rev.* E **66** 016614
[17] Gaeta G 1994 *Phys. Lett.* A **190** 301
Gaeta G 2006 *Phys. Rev.* E **74** 021921
[18] Mingaleev S F, Christiansen P L, Gaididei Yu B, Johanson M and Rasmussen K Ø 1999 *J. Biol. Phys.* **25** 63
Gaididei Yu B, Mingaleev S F, Christiansen P L and Rasmussen K Ø 1997 *Phys. Rev.* E **55** 6141
[19] Dauxois T, Peyrard M and Bishop A R 1993 *Phys. Rev.* E **47** R44
Barbi M, Cocco S and Peyrard M 1999 *Phys. Lett.* A **253** 358
[20] Barbi M, Cocco S, Peyrard M and Theodorakopoulos N 2003 *Phys. Rev.* E **68** 061909
[21] Zdravkovič S and Satarič M V 2007 *Europhys. Lett.* **78** 38004
Zdravkovič S and Satarič M V 2007 *Chin. Phys. Lett.* **24** 1210
Zdravkovič S and Satarič M V 2005 *Chin. Phys. Lett.* **22** 850
[22] Tabi C B, Mohamadou A and Kofane T C 2008 *J. Comput. Theor. Nanosci.* **5** 647
Mohamadou A, Kenfack A J and Kofane T C 2005 *Phys. Rev.* E **72** 036220
Nguenang J P, Peyrard M, Kenfack A J and Kofane T C 2005 *J. Phys.: Condens. Matter* **17** 3083
[23] Sulem C and Sulem P L 1999 *The Nonlinear Schrodinger Equation* (New York: Springer)
[24] Peyrard M, Boesch R and Kourakis I 1991 Collective proton transport in hydrogen bonded systems *Proc. NATO Advanced Research Workshop (Heraklion, Crete)* ed T Bountis (New York: Plenum)
[25] Taniuti T and Washimi H 1968 *Phys. Rev. Lett.* **21** 209
Hasegawa A 1970 *Phys. Rev. Lett.* **24** 1165
Hasegawa A 1971 *Phys. Fluids* **15** 870
[26] Marquié P, Bilbaut J M and Remoissenet M 1994 *Phys. Rev.* E **49** 828
Marquié P, Bilbaut J M and Remoissenet M 1995 *Phys. Rev.* E **51** 6127
Ndzana F II, Mohamadou A and Kofané T C 2007 *J. Phys. D: Appl. Phys.* **40** 3254
[27] Bespalov V I and Talanov V I 1966 *Pis. Zh. Eksp. Teor. Fiz.* **3** 471
Bespalov V I and Talanov V I 1966 *JETP Lett.* **3** 307 (Engl. Transl.)
[28] Dauxois T 1991 *Phys. Lett.* A **159** 390

Calvo G F and Alvarez-Estrada R F 2008 *J. Phys.: Condens. Matter* **20** 035101
[29] Dauxois T and Peyrard M 1993 *Dynamics of Breathers Modes in a Nonlinear Helicoidal Model of DNA* (*Lecture Notes in Physics* vol 393) ed M Remoissenet and M Peyrard (Berlin: Springer) pp 76–86
[30] Barbi M, Cocco S, Peyrard M and Ruffo S 1999 *J. Biol. Phys.* **24** 97
[31] Barbi M 1998 *PhD Thesis* University of Florence
Cocco S 2000 *PhD Thesis* University of Rome-La Sapienza and ENS-Lyon
[32] Strick T *et al* 2000 *Physica* A **263** 392
Strick T *et al* 1996 *Science* **271** 1835
[33] Barbi M, Lepri S, Peyrard M and Theodorakopoulos N 2003 *Phys. Rev.* E **68** 061909
[34] Kivshar Y S and Peyrard M 1992 *Phys. Rev.* A **46** 3198
[35] Daumont I, Dauxois T and Peyrard M 1997 *Nonlinearity* **10** 617
[36] Zakharov V E and Shabat A B 1972 *Sov. Phys.—JETP* **34** 62
[37] Akhmediev N N and Ankiewicz A 1997 *Solitons: Nonlinear Pulses and Wavepackets* (London: Chapman and Hall)
[38] Vazquez L, Streit L and Perez-Garcia V M (ed) 1996 *Nonlinear Klein–Gordon and Schrodinger Systems: Theory and Applications* (Singapore: World Scientific)
[39] Sulem C and Sulem P 2000 *The Nonlinear Schrödinger Equation: Self-focusing and Wave Collapse* (Berlin: Springer)
[40] Hasegawa A and Tappert F 1973 *Appl. Phys. Lett.* **23** 142
[41] Peyrard M 1998 *Physica* D **119** 184
[42] Bang O and Peyrard M 1996 *Phys. Rev.* E **53** 4143
[43] Tsironis G P, Bishop A R, Savin A V and Zolotaryuk A V 1999 *Phys. Rev.* E **60** 6610
[44] Kapri R and Bhattachrjee M S 2007 *Phys. Rev. Lett.* **98** 098101
Zamora-Sillero E, Shapovalov A V and Esteban F J 2007 *Phys. Rev.* E **76** 066603